LCADNet: A Novel Light CNN Architecture for EEG-based Alzheimer Disease Detection

Pramod Kachare[1], Digambar Puri[1], Sandeep B. Sangle[1], Ibrahim Al-Shourbaji[2,3], Abdoh Jabbari[2], Raimund Kirner[3], Abdalla Alameen[4], Hazem Migdady[5] and Laith Abualigah[6*]

[1]Department of Electronics and Telecommunication, Ramrao Adik Institute of Technology, D. Y. Patil Campus, Navi-Mumbai, 400706, Maharashtra, India.
[2]Department of Computer & Network Engineering, Jazan University, Jazan, Saudi Arabia.
[3]Department of Computer Science, University of Hertfordshire, Hatfield, , UK.
[4]Department of Computer Science, College of Arts and Sciences, Prince Sattam Bin Abdulaziz University, Saudi Arabia.
[5]CSMIS Department, Oman College of Management and Technology, 320 Barka, Oman.
[6]Department of Computer Science , Al al-Bayt University, Mafraq Jordan.

*Corresponding author. E-mails: aligah@usm.my;

Abstract

Alzheimer's disease (AD) is a progressive and incurable neurological disorder with a rising mortality rate, worsened by error-prone, time-intensive, and expensive clinical diagnosis methods. Automatic AD detection methods using hand-crafted Electroencephalogram (EEG) signal features lack accuracy and reliability. A lightweight convolution neural network for AD detection (LCADNet) is investigated to extract disease-specific features while reducing the detection time. The LCADNet uses two convolutional layers for extracting complex EEG features, two fully connected layers for selecting disease-specific features, and a softmax layer for predicting AD detection probability.

A max-pooling layer interlaced between convolutional layers decreases the time-domain redundancy in the EEG signal. The efficiency of the LCADNet and four pre-trained models using transfer learning is compared using a publicly available AD detection dataset. The LCADNet shows the lowest computation complexity in terms of both the number of floating point operations and inference time and the highest classification performance across six measures. The generalization of the LCADNet is assessed by cross-testing it with two other publicly available AD detection datasets. It outperforms existing EEG-based AD detection methods with an accuracy of **98.50%**. The LCADNet may be a valuable aid for neurologists and its Python implementation can be found at github.com/SandeepSangle12/LCADNet.git.

Keywords: Electroencephalogram; Alzheimer's disease; Convolution neural network; Pre-trained models

1 Introduction

Alzheimer's disease (AD) is the most common type of dementia in the elderly and is warned to affect more than 130 million people by 2050 [1]. AD can be characterized by cognitive dysfunctions, aphasia, poor judgment, memory loss, and several difficulties in daily activities [2]. Mild cognitive impairment (MCI), an initial AD stage, occurs in $5-20\%$ of elderly (>60 years) with symptoms that are overlapping symptoms with typical aging signs [3, 4]. Although AD is incurable to date, medications can delay the severe stage of AD [5]. Proper precautions can aid AD patients to maintain independence for a longer duration and delay depression and social costs [6].

Clinically, AD is diagnosed by various blood, neurological, and psychological tests, which are subjective and demand the expert neurologist [7]. Various neuroimaging methods, such as single-photon emission computed tomography, magnetic resonance imaging (MRI), and positron emission tomography, used to detect AD are time-consuming, expensive, and radiogenic [8]. A safer approach investigates Electroencephalogram (EEG) for detecting brain abnormalities observed in AD patients. EEG-based automatic AD detection systems have a high temporal resolution, low cost, and non-invasive implementation [9]. AD patients show more slowing, decreased synchrony, and reduced complexity of EEG signals than normal controlled (NC) subjects [10].

Literature reports several models for two-way (AD vs NC, AD vs MCI, and NC vs MCI) or three-way (AD vs MCI vs NC) classification by extracting EEG-based discriminating features [11]. In [12], the coherence and spectral power as distinct feature sets with support vector machine (SVM) resulted in 91.4% AD detection accuracy. In [13], biomarkers based on approximate entropy (ApEn), fuzzy entropy (fuEn) [14], Kolmogorov complexity [15], and auto mutual information (AMI) reported AD detection accuracy of 91.9%. In [16], an SVM classifier is trained using a combination of sample entropy

(SampEn) [17], AMI, and spectral entropy (SpEn) [17] with median frequency and band power. However, these reported results are not consistent. In [18], multiscale entropy (MSEn) [19] and canonical correlation analysis reported an accuracy of 79.49% using logistic regression (LR). However, two-way AD vs NC classification performance was variable. In [20], a combination of SpEn, power spectral density (PSD), Higuchi's fractal dimension, spectral crest factor, kurtosis, and skewness achieved an accuracy of 89%. Most of these features are affected by the signal length and different input parameters.

In [21], time-frequency and spectral domain biomarkers for AD from NC subjects are classified using k-nearest neighbour (KNN) to obtain 97% accuracy. They reported higher perturbation in EEG synchrony of AD patients compared to NC subjects [21]. Farina *et al.* [22] combined MRI and EEG to calculate functional connectivity and band power features along with the mini-mental state examination score (MMSE) to detect AD subjects. Oltu *et al.* [23] trained an efficient SVM classifier using DWT-based PSD and coherence features to detect AD from MCI and NC with the accuracy of 97%. Pirrone *et al.* [24] calculated the power difference of subbands, obtained by finite impulse response filtering with cut-off frequencies 7 and 16 Hz. A three-way classification using these features and an SVM model reported 86% accuracy. Swarnalatha [25] detected AD stages (severe, moderate, and mild) using a deep learning (DL) model based on a hybrid greedy sandpiper approach. Although the model obtained the best accuracy of 99.8%, it does not apply to other open-source datasets [25].

Most of the reported studies in the literature used the Empirical mode decomposition (EMD), Fast Fourier Transform (FFT), wavelet decomposition, and nonlinear algorithms to detect AD, which depends on the order of filters, window selection, and wavelets. The selection of decomposition parameters for EMD, variational mode, discrete (DWT) and tunable-Q wavelet decomposition is tedious due to non-stationary EEG signals. Nonlinear techniques, like entropy-based, are parameter-dependent. Therefore, selecting the salient parameters is challenging. Moreover, traditional signal processing techniques are time-consuming and demand substantial quantitative and qualitative parametric analysis that directly controls the system's accuracy.

Various DL models reported to detect AD are presented in Table 1. Nour *et al.* [26] investigated the ensemble deep model with convolution neural network (CNN). In [27], PSD-based biomarkers and long-short-term memory (LSTM) with adaptive parameters for classification. Miltiadous *et al.* [28] investigated band power and spectral coherence connectivity for AD detection. Although the success of UNet architecture in computer vision motivates its use for AD detection, larger CNNs like UNet and several others reported in the literature increase computational complexity and memory requirements during training and test phases. Also, the inference time required is much higher due to the number of floating-point calculations involved in such models. Hence, there is a need for a lightweight model with a shorter inference time and higher or comparative detection performance than earlier reported models in the literature.

Table 1: The state-of-the-art EEG-based AD detection methods using CNN models

Reference	Year	Features	Channels	Subjects	Classifier	ACC (%)	SEN (%)	SPE (%)
Nour *et al.* [26]	2024	Ensemble DL model	19	24 AD, 24 NC	CNN	97.90	98.23	98.68
Siuly *et al.* [27]	2024	PSD based biomarkers	20	51 AD1, 35 NC	LSTM	97.00	97.48	96.48
Miltiadous *et al.* [29]	2023	Band power, Spectral coherence connectivity	19	36 AD, 29 NC	Dual input CNN	83.28	78.81	87.94
Calub *et al.* [29]	2023	Linear & non-linear Uni-variate features + PCA	21	31 AD, 20 MCI, 35 NC	KNN	97.64	95.40	98.81
Fouad *et al.* [30]	2023	Constrast, homogeneity, & wavelet statistics	19	59 AD, 7 MCI, 102 NC	ResNet	97.82	97.83	98.26
Ho *et al.* [31]	2022	ERSP features	19	23 NC, 40 AD	CNN-LSTM	75.95	77.23	69.40
Alvi *et al.* [32]	2022	EEG Spectrogram	19	11 NC, 16 AD	LSTM	96.91	97.95	96.16
Toural *et al.* [33]	2020	Wavelet entropy & band-power	19	17 NC, 9 MCI, 15 AD	SVM	AD vs. NC: 93.33 MCI vs. NC: 88.88	96.15 100	95.12 97.56

ERSP - event-related spectral perturbation, PCA-principle component analysis, RUS-Random undersampling.

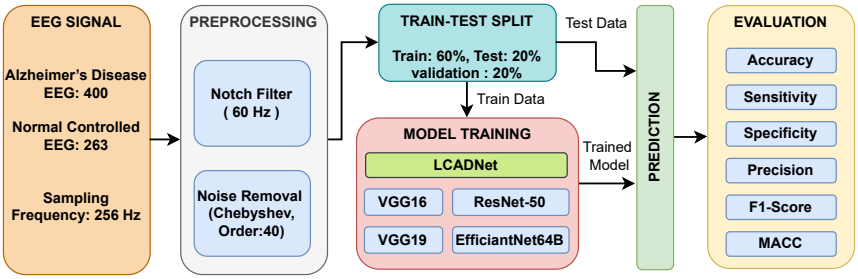

Fig. 1: Schematic flow of proposed work.

An EEG-based automatic AD detection system using CNN is proposed for reducing the computation complexity while achieving high detection accuracy. The computation complexity is proportional to the number of trainable parameters in the CNN model. An automatic AD detection system using a CNN with the least number of weighted layers and a spatio-temporal representation of the EEG signal is presented. The contributions of the presented work are:

- The LCADNet, a low computation complexity CNN model, is presented for improving the EEG-based automatic AD detection system using a publicly available dataset.
- The LCADNet uses convolutional layers to extract complex features, a max-pooling layer to reduce redundancy, fully connected layers to select salient features, and a softmax layer to generate AD detection probability.
- Classification performance and computation complexity of the LCADNet is compared with pre-trained models and existing AD detection methods.
- The LCADNet layers are visualized for discriminating AD and NC EEG signals and generalization is supported by cross-testing with other datasets.

The organization of the paper is as follows. The proposed methodology is described in section 2. Experimental results are discussed in section 3. A Proposed model and comparison with the state-of-the-art methods is discussed in section 4. The conclusion is given in section 5.

2 Methodology

The application of the CNN model allows for intricate pattern recognition in EEG signals, enhancing the precision and reliability of AD detection. A schematic of EEG-based the automatic AD detection system is presented in Fig. 1. The dataset, preprocessing, the lightweight CNN architecture, and evaluation measures are explained in the following sections.

2.1 EEG Dataset and Preprocessing

The dataset comprises EEG signals from 12 AD patients (7 female and 5 male) and 11 NC subjects (7 female and 4 male). All AD patients belonged to

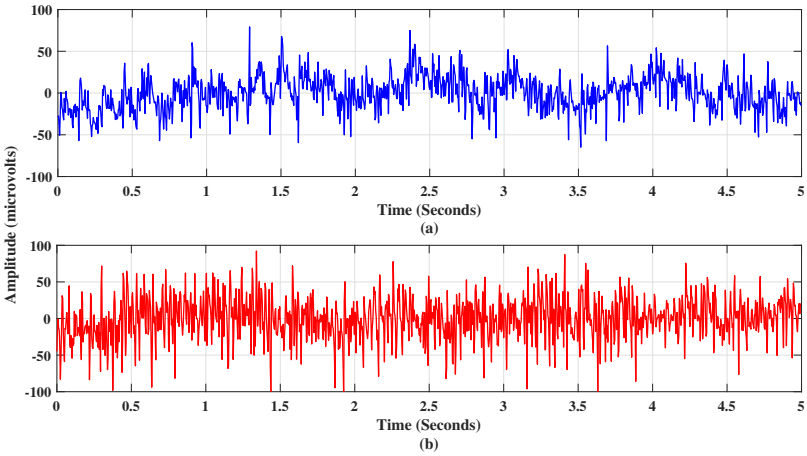

Fig. 2: An example of preprocessed EEG signal for (a) AD and (b) NC subjects.

the Association of Alzheimer's Patients Relatives (AFAVA), Valladolid, Spain. Subjects were checked before recruitment for the presence of undesired neurological disorders like epilepsy, Parkinson's disease, etc. AD patients had an average MMSE score of 13.1 and standard deviation of 5.9 and NC subjects scores were greater than 30. The signals were recorded for five seconds using Oxford Instruments' 2.3.411 EEG profile study room system using International $10-20$ electrode placement system with electrodes C_z, C_3, C_4, F_3, F_4, F_7, F_8, F_z, Fp_1, Fp_2, O_1, O_2, P_z, T_3, T_4, T_5, T_6, and earlobes reference points.

The EEG recordings were digitized using a 12-bit analog-to-digital converter at 256 Hz sampling frequency. The EEG signal was filtered using the 40th order Chebyshev bandpass ($0.5-100$ Hz) filter to reduce the noise and notch filter with 60 Hz cut-off frequency to eliminate powerline supply frequency. An example AD and NC EEG signals for C_z electrode is shown in Fig. 2. In the experimental setup, each EEG signal was preprocessed individually to remove artifacts, resulting in 9849 recordings for analysis, 5648 from the AD class and 4201 from the NC class [34]. The dataset of the processed signals is made publicly available by the University of Edinburgh (datashare.is.ed.ac.uk/handle/10283/2783) [35]. A summary of AD and NC EEG signal characteristics is presented in Table 2.

2.2 Low-complexity CNN

The study aims to design a CNN for AD detection with faster prediction, low memory usage, and low training time. These requirements can be achieved by minimizing the number of trainable parameters in the CNN. This section describes the LCADNet, a low-complexity CNN for automatic AD detection. Fig. 3 shows architectural details of the proposed LCADNet for binary-class

AD detection. The architecture can be grouped into two parts [36]: (i) feature extractor (input to flatten layers) and (ii) classifier (flatten to output layers).

The feature extraction part of the LCADNet generates a high-dimension feature representation of AD and NC EEG signals. It uses spatio-temporal EEG data as input and four layers. The input EEG data has 16 electrodes and a sequence of 1280 voltage values, as described earlier in the section 2.1. Hence, the shape of LCADNet input data is (16, 1280). The feature extraction part has two convolutional (Conv2D) layers, a max-pooling (MaxPool2D) layer, and a flatten layer. The Conv2D layers learn kernel weights suitable to generate complex disease-specific features [36]. The first Conv2D layer has 3×3 kernels to generate coarse features by combining the input spatio-temporal EEG signal.

The low-frequency components in the EEG signals are most informative, leading to intrinsic redundancy within the temporal sequence. The max-pooling is strategically used to capture relatively higher temporal redundancy in the EEG signal. It selects the most excited patterns in the EEG signal and increases the span of convolution calculation [36]. For the output of previous layer $F(.)$, the MaxPool2D layer output $g_{max}(.)$ is calculated as

$$g_{max}(a,b) = max\left[F(h,v), F(h+1,v), F(h,v+1), F(h+1,v+1)\right] \quad (1)$$

Table 2: A summary of AD and NC EEG signal characteristics.

Parameters	AD	NC
No. of subjects	12	11
Age	72.8 ± 8 years	72.5 ± 6.1 years
Avg. trials per subject	34	24
No. of EEG recordings	400	263
Sampling Frequency	256 Hz	256 Hz
Length of each recording	5 sec (1280 samples)	5 sec (1280 samples)
No. of channels	16	16

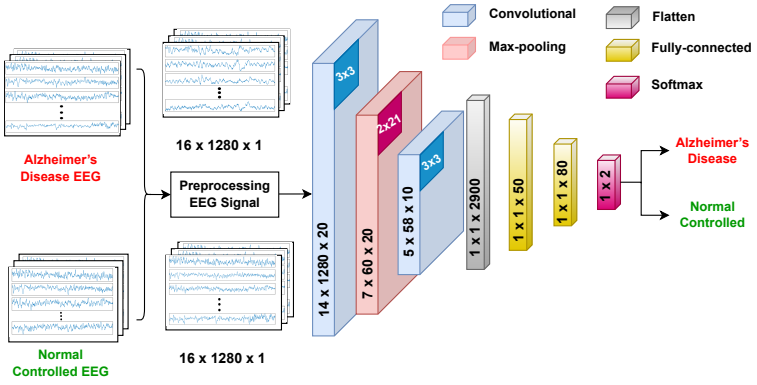

Fig. 3: Proposed LCADNet model for Alzheimer's disease detection.

Table 3: An architectural summary of the LCADNet model

Layer	Output Shape	Kernal Shape	Parameters
Input	16, 1280, 1	-	-
Conv2D	14, 1278, 20	3×3	200
MaxPool2D	7, 60, 20	2×21	0
Conv2D	5, 58, 10	3×3	1810
Flatten	2900	-	0
FC	50	-	145050
FC	80	-	4080
Softmax	2	-	162
Trainable parameters			1,51,302

where $h = a+s$ and $v = b+s$. Here, a, b are horizontal and vertical indices and s is stride. The MaxPool2D layer has 2×21 kernels to extract max values from the output feature map of the previous convolutional layer.The asymmetric kernel size captures higher temporal redundancy and reduces the temporal dimension by a large factor for extracting the most important features. It is followed by another Conv2D layer to generate more complex spatio-temporal features. Finally, a flatten layer transforms a multi-dimension spatio-temporal feature map of the EEG data into a feature vector. The dimension of the feature vector is a product of the dimensions of the output feature map of the last convolutional layer. The classifier part of the LCADNet further processes the output of the feature extractor.

The classifier part of the LCADNet comprises two fully-connected (FC) layers to select the most important features while achieving nonlinear transformation of feature vector and a softmax layer to generate AD detection probability. The bottleneck architecture with two consecutive FC layers each having 50 and 80 neurons reduces the computational complexity exponentially due to decreased trainable parameters of these layers [36]. The softmax layer generates probabilistic scores for output binary classes. The softmax layer transforms the output of the fully connected layer into a probability distribution, assigning a likelihood to each potential class. It enables AD detection and a nuanced understanding of the model's confidence in its predictions, contributing to interpretability and reliability of the AD detection system.

The details of the output shape, kernel size, and the number of trainable parameters of the proposed LCADNet are provided in Table 3. In terms of number of trainable parameters, pooling and flatten layers do not contribute anything. The compression achieved by the asymmetric kernel size in the pooling reduced the feature map input to the following convolutional layer and hence, it aided in reducing the overall trainable parameters of the model. The FC layers has the highest number of trainable parameters, approximately 98.56 % of the total trainable parameters. The two convolutional layers contribute fewer trainable parameters. The number of trainable parameters of the softmax layer depend on the number of output classes.

An adaptive moment estimation (Adam) optimizer is used to update the network weights iteratively. It simplified each weight's learning rate in the network by combining the root mean square propagation and stochastic gradient descent. For a given m^{th} training sample, $y_p(m,k)$ is the k^{th} predicted probability value $\sum_k y_p(m,k) = 1, \forall m$. The cross-entropy loss (L) is used to train the model and it can be expressed as [36]:

$$L = -\sum_{m-1}^{N_t}\sum_{k-1}^{N_c} y(m,k) \times \log y_p(m,k) \tag{2}$$

where N_t is the number of training samples and and N_c is number of classes.

2.3 Evaluation Metrics

The AD detection ability of different DL models is evaluated using accuracy (ACCU), sensitivity (SENS), specificity (SPEC), precision (PREC), F1-score (F1), and Matthew's correlation coefficient (MACC). These parameters are calculated as [37, 38]:

$$ACCU = \frac{S_{pp} + S_{nn}}{S_{pp} + S_{pn} + S_{pn} + S_{nn}} \times 100 \tag{3}$$

$$SENS = \frac{S_{pp}}{S_{pp} + S_{pn}} \times 100 \tag{4}$$

$$SPEC = \frac{S_{nn}}{S_{nn} + S_{np}} \times 100 \tag{5}$$

$$PREC = \frac{S_{pp}}{S_{pp} + S_{np}} \times 100 \tag{6}$$

$$F1 = \frac{2 \times PREC \times SENS}{PREC + SENS} \times 100 \tag{7}$$

$$MACC = \frac{S_{pp} \times S_{nn} - S_{pn} \times S_{np}}{[(S_{pp} + S_{np})(S_{pp} + S_{pn})(S_{nn} + S_{pn})(S_{nn} + S_{pn})]^{0.5}} \times 100 \tag{8}$$

Here, S_{ij} is the subject actually from ith class and predicted as jth class, where $i, j \in \{p, n\}$ indicating AD and NC subjects, respectively.

3 Results

The experiments are conducted on a computer with a 1.32 GHz processor, a Nvidia P100 GPU, 16 GB of RAM, and a Linux Operating system. The LCADNet is implemented in Python using TensorFlow and Keras libraries. For comparison, the transfer learning approach is used to adjust the classifier part of the pre-trained CNN models comprising VGG16, VGG19, ResNet50, and EfficientNetB4. The classifier part of the pre-trained models and the LCADNet are kept the same to compare their feature extraction capabilities.

3.1 Hyper-parameter Tunning

All models used the Adam optimizer with an initial learning rate of 0.0001. A systematic grid search tunes the batch size and epoch of the LCADNet and the pre-trained CNNs. The batch size is searched linearly from 50 to 200 in steps of 5 and the number of epochs is searched linearly from 50 to 300 in steps of 10. The LCADNet, EfficientNetB4, and RestNet performed best for a batch of 80 examples. The VGG 16 and VGG19 showed the best performance for batch sizes 120 and 110, respectively. The maximum number of epochs is set at 100 for all models. Despite a slight inconsistency in epoch values, they are retained as these yielded optimal AD detection performance, ensuring fair competition of all models.

3.2 Comparision with Pre-trained CNNs

ALL EEG recordings are randomly grouped into three mutually exhaustive and exclusive subsets for training, validation, and testing as 60%, 20%, and 20%, respectively. Four pre-trained CNN models and the LCADNet performances are compared using the metrics described in Section 2.3 and are presented in Table 4. The LCADNet demonstrates remarkable performance across all dataset groups and evaluation metrics for AD detection. It consistently outperforms competing models, including VGG16, VGG19, ResNet50, and EfficiantNetB4, achieving high accuracy, sensitivity, specificity, and precision. LCADNet achieves perfect accuracy during training and maintains superior performance in the validation and testing phases. The MACC surpasses the F1 score and accuracy in providing valuable insights when assessing binary classification problems, as it factors in the distribution balance among the four categories in the confusion matrix. As shown in Table 4, the LCADNet outperforms other pre-trained models.

The convergence of all models is analyzed to learn the stability of models over different number of epochs. Fig. 4 and 7 depict all the model's accuracy and loss plots over the number of epochs. These accuracy and loss curves show the convergence over time as the model learns from the data. This convergence indicates that the model is improving and approaching an optimal solution. The accuracy and loss curve of VGG-16 and ResNet50, In Fig. 4 and 6 indicate the dissimilarities between all epochs of training and validation curve compared to other model's accuracy and loss curves. Similarly, for the VGG-19 and the

Table 4: Performance evaluation using different models and LCADNet

Model	Dataset	ACCU (%)	SENS (%)	SPEC (%)	PREC (%)	F1 (%)	MACC (%)
VGG16	Training	94.55	94.59	94.56	94.56	94.58	89.12
	Validation	92.45	92.52	92.45	92.45	92.48	84.91
	Testing	96.24	95.00	98.11	98.70	96.82	92.33
VGG19	Training	94.97	95.34	95.28	95.28	95.31	96.23
	Validation	98.11	98.19	98.11	98.11	98.15	96.23
	Testing	96.99	97.48	96.43	97.42	97.45	93.83
ResNet50	Training	99.24	98.97	98.97	98.97	98.97	97.95
	Validation	96.23	96.35	96.23	96.45	96.40	92.45
	Testing	96.99	98.67	94.83	96.10	98.02	93.91
EfficiantNetB4	Training	82.18	82.19	82.19	82.19	82.19	64.37
	Validation	84.91	84.95	84.92	84.91	84.93	69.81
	Testing	88.72	90.80	93.48	96.34	93.49	82.45
LCADNet	Training	100	100	99.84	99.79	99.89	100
	Validation	99.06	99.26	99.15	99.40	99.33	98.11
	Testing	98.50	100	97.55	97.40	98.68	96.98

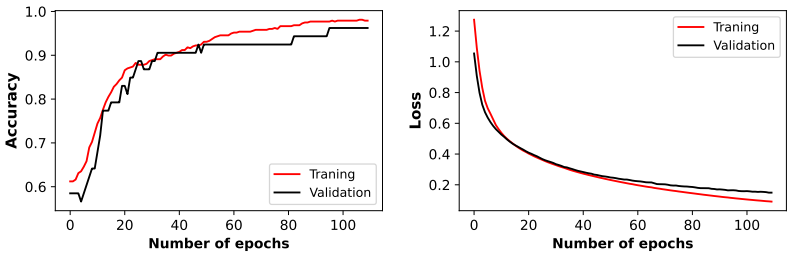

Fig. 4: Accuracy and loss curve of training and validation data using VGG16.

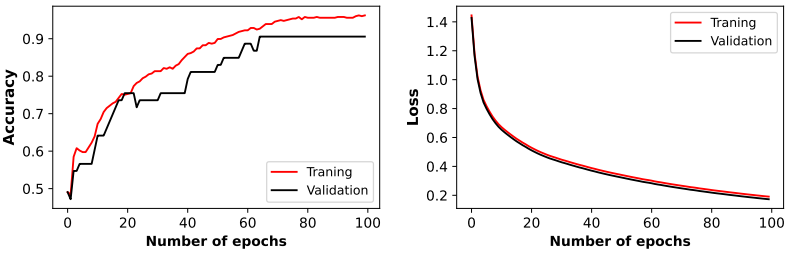

Fig. 5: Accuracy and loss curve of training and validation data using VGG19.

LCADNet, Fig. 5 and 8 shows the difference between 0 to 25 epochs and 5 to 15 epochs, respectively. The accuracy and loss curve of the EfficientNetB4

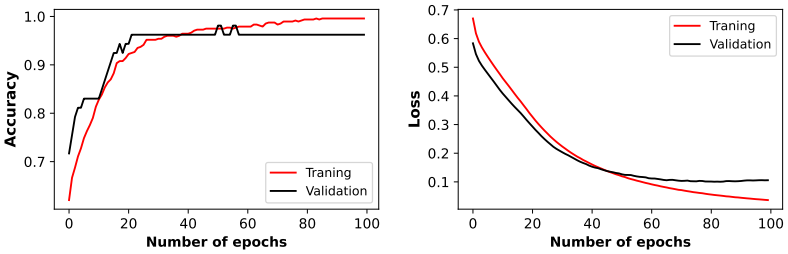

Fig. 6: Accuracy and loss curve of training and validation data using ResNet50.

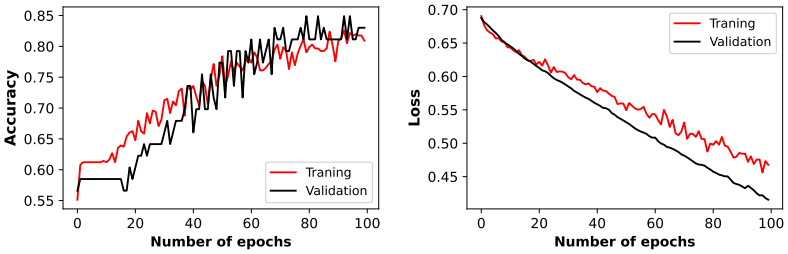

Fig. 7: Accuracy and loss curve of training and validation data using EfficientNetB4.

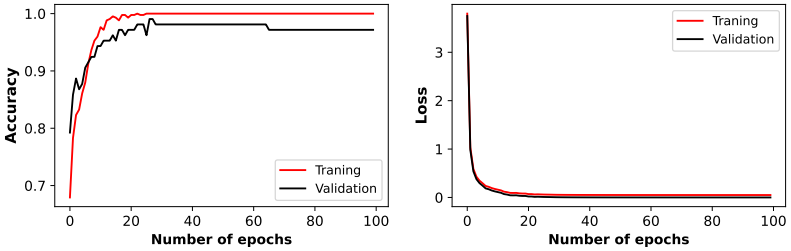

Fig. 8: Accuracy and loss curve of training and validation data using proposed LCADNet.

is continuous in fluctuations. This fluctuation can occur due to the stochastic nature of specific algorithms.

3.3 Computation Complexity

A complex model is necessary to capture patterns in the EEG signal, too much complexity may lead to overfitting. The total number of parameters in each model is directly related to the computation complexity of the model.

Table 5: Comparison of computation complexity of different models.

Model	Parameters	GFLOPS	Inference Time (ms)
VGG16	1,47,44,580	12.535	0.466
VGG19	2,00,54,276	15.933	0.304
ResNet50	2,36,94,404	3.164	0.226
EfficiantNetB4	1,77,67,715	1.257	0.395
LCADNet	1,51,302	0.009	0.064

VGG19 has more parameters than VGG16 and EfficientNetB4. The ResNet50 has the highest number of trainable parameters among the five CNN models and LCADNet has the lowest number of trainable parameters. Giga Floating Point Operations per Second (GFLOPs) [39], the total number of floating point multiplications and additions per second, and inference time, the time the model takes to generate a prediction for new input data, are the two most commonly known quantitative measures for computation complexity. As reported in Table 5, LCADNet is the most efficient model with the smallest GFLOPS of 0.009 and the shortest inference time of 0.064 sec. Based on computational efficiency during inference, emphasizing its suitability for real-time applications.

3.4 Layer Visualization

The flattened layer data distribution plots of VGG16, VGG19, ResNet50, EfficientNetB4, and LCADNet are depicted in Fig. 9. The flattened layer is used to transform multi-dimensional data into a one-dimensional array. This operation is typically applied before feeding the data into a fully connected layer,

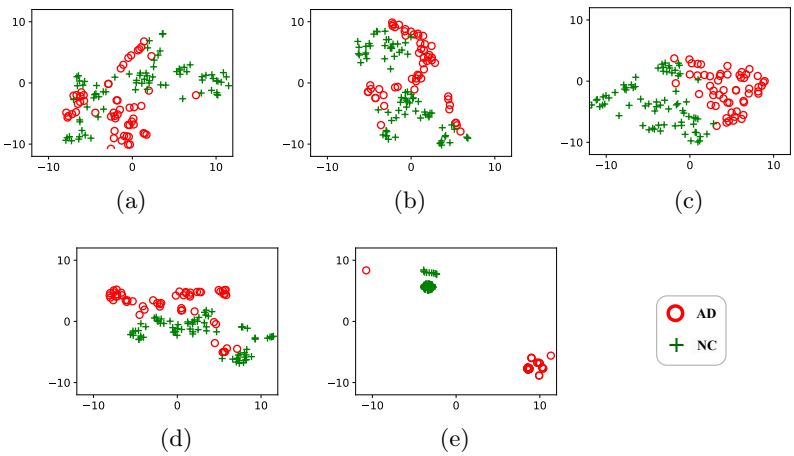

Fig. 9: A t-SNE visualization of feature extractor part of (a) VGG16, (b) VGG19, (c) ResNet-50, (d) EfficientNetB4, and (e) LCADNet.

which requires one-dimensional input. So, the flattened layer plays a vital role in the model to observe the model's behaviour and complexity. Flatten layer data is distributed using the t-distributed stochastic neighbour embedding (t-SNE) for visualizing data. This data distribution shows both class samples with different colors. The complexity of the model can be observed through that distribution plot. Except for the EfficientNetB4, all the models of the distribution plots can be separated easily.

Fig. 10 shows a feature map of the LCADNet convolutional layer for AD and NC class samples. Visualizing convolution feature maps in EEG signals provides valuable insights into the learned representations within CNN. The feature maps revealed altered patterns in the AD samples compared to the NC sample. These indicate potential biomarkers and neuro-physiological changes specific to AD. The figure's number of rows and columns indicates the convolutional layer and class, respectively. In Fig. 10, the values on the x and y-axis indicate the EEG channel and EEG time samples, respectively. The value of the EEG channel and EEG time samples are the same as the output shape of LCADNet, as shown in Table 3.

In the feature map of the first convolutional layer, high activation values for AD samples are observed at the zero position of the EEG channel. In contrast, NC samples appear in the fifth position. The activations are contributed by the filter of the first layer, which detects relevant features in both the AD and NC samples. Lower values suggest that the kernels did not respond strongly to the remaining regions of the input. In the second CNN layer, for AD samples, the higher value band is observed at the 1st of the EEG channel, while the lower value band is at the 5th EEG channel. The higher value band is seen

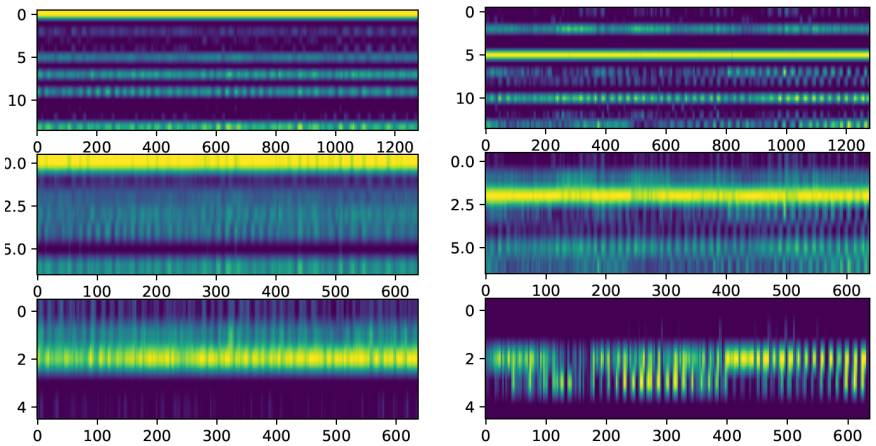

Fig. 10: Visualization of LCADNet layers feature maps for (a) AD and (b) NC samples. Each row represents an LCADNet layer, and each column represents a class (AD or NC).

at the 3rd EEG channel for NC samples. In this layer, the higher value band becomes wider than the first. The lower value bands in the third CNN layer are precisely opposite each other with respective classes. The higher values are continuously observed at the 2nd EEG channel for AD samples, but they are mixed with lower values for NC samples. Through the visualization of feature maps, it is possible to observe distinctive patterns that can aid in distinguishing between the AD and NC classes. The feature maps highlight the regions of the input data that are important for classification and become more abstract and informative as the network processes for deeper layers.

3.5 Model Generalization

For analyzing the generalization of the LCADNet model, cross-testing is done using two additional datasets. Details of dataset A are given in section 2.1. The publicly available dataset B [40] comprises three classes (AD/MCI/NC) and is recorded from 213 subjects (59 AD, 70 MCI, and 102 NC) in a similar age group as dataset A. Each class has approximately equal proportions of male and female subjects. Each EEG signal is 7.8 sec and recorded at 256 Hz. Another dataset C [41] is an open-access three-class (FTD/AD/NC) dataset from OpenNeuro recorded from 85 subjects (33 MCI, 23 AD, and 29 NC). Each signal was downsampled to 256 Hz and lasted approximately 13.5 minutes for AD, 12 minutes for FTD, and 13.8 minutes for NC. The EEG signals corresponding to AD and NC from both datasets are segmented into 5-sec signals and 16 EEG channels as described in Section 2.1 are selected out of 19 available channels.

The LCADNet is trained using each dataset separately and evaluated using all three datasets.Table 6 shows the auto and cross-testing performance of the LCADNet model using all three datasets. This table provides insights into how the performance of the LCADNet model varies when trained and tested on different datasets, highlighting the importance of dataset selection and generalization of the model. The results show that the LCADNet demonstrates strong performance across all datasets in terms of ACCU and F-score. For Dataset A, the model achieves consistently high accuracy and F1 scores across different tests, indicating robust performance and good generalizability. For Dataset B, the model maintains high accuracy and F1 scores during both training and testing, suggesting its ability to generalize well to unseen data. For Dataset C, although the accuracy and F1 scores are slightly lower compared

Table 6: Performance of LCADNet model using Dataset A and B

Test	A		B		C	
Train	ACCU	F1	ACCU	F1	ACCU	F1
A	98.50	98.68	94.39	96.43	92.12	93.65
B	96.24	96.64	99.49	99.70	92.62	92.56
C	91.64	92.79	92.56	93.65	93.14	95.76

to the other datasets, the model still performs reasonably well, indicating the generalizability to this dataset.

4 Discussion

This study proposes the LCADNet model and compares performance with pre-trained transfer learning models. Transfer learning is defined as training a neural network on a new task using the weights of another task; the new model doesnt need to be prepared from scratch. The Proposed LCADNet model used much less parameters and low complexity to outperform the huge pre-trained model. The first reason is that the input layer of the LCADNet model is trained on one channel, while the pre-trained model is pre-trained on the 3-channel ImageNeT dataset. The second reason is that several layers are used in the pre-trained and LCADNet models, which affect the complexity of the model.

In this study, pre-trained models are used in the ImageNet dataset and tested on EEG signals. Generated weights of pre-trained models do not outperform LCADNet in distinguishing between AD and NC EEG signals. While the LCADNet model is trained and tested on the same dataset, it makes a task-specific model for AD and NC classification and outperforms other models.

Overall, these results highlight the potential of the LCADNet model and spatio-temporal features in distinguishing EEG signals between AD and NC subjects. The visualizations contribute to developing objective and quantitative methods for AD diagnosis and monitoring. In this study, the CNN architecture used a binary classification setup with two neurons at the last layer utilizing the softmax activation function. Importantly, our design allows straightforward adaptation to multi-class classification with N classes; the number of neurons in the last layer should be adjusted to N, providing a flexible and scalable solution.

4.1 Comparison with Existing Models

The comparative analysis of the proposed LCADNet and state-of-the-art techniques using the AFAVA dataset is presented in Table 7. Several EEG-based automatic AD detection models are reviewed earlier in section 1. Abasolo *et al.* [17] reported 77.27% classification accuracy using SpEn and SampEn features. Similarly, the multiscale entropy features with student's t-test have been presented by Escudero in [42]. The classification accuracy has been enhanced to 95.45% using ApEn, AMI, detrended moving average, and detrended fluctuation analysis (DFA) [43]. However, the models reported by Abasolo *et al.* [17] and Escudero in [42] are limited by the parametric and time-varying entropy-based methods. Simon *et al.* [44] investigated the quadratic SpEn, generalized MSE, distance-based LZC [34], and fuEn [14] for detecting AD with Mann-Whitney U-test and Lillifors test with the AD detection accuracy of 86.36%. Most methods reported in Table 7 have utilized time-dependent features. Hence, there is a missing frequency domain information. The wavelet-based

Table 7: Performance comparison of present work with previously existing techniques that have used ***same*** AD-EEG dataset (AFAVA dataset).

Reference	Year	Method	ACCU (%)	SENS (%)	SPEC (%)
Escudero *et al.* [42]	2006	MSEn features	90.91	90.91	90.91
Abasolo *et al.* [17]	2006	SpEn and SampEn features	77.27	90.91	63.64
Abasolo *et al.* [49]	2008	ApEn and AMI	90.91	100	81.82
Abasolo *et al.* [43]	2008	DFA - LDA	95.45	90.91	100
Abasolo *et al.* [50]	2009	DMA	81.82	90.91	72.73
Simons *et al.* [44]	2015	Q-SpEn	77.27	79.19	77.97
Azami *et al.* [19]	2017	GMSEn Mann-Whitney test	72.73	75.86	80.68
Simons *et al.* [34]	2017	Lempel Ziv complexity	77.27	72.73	81.82
Simons *et al.* [14]	2018	FuzzyEn with Lillifors test	86.36	81.82	90.91
Puri *et al.* [51]	2022	EMD with Hjorth Parameters	92.90	94.32	94.34
Present work	2024	LCADNet Model	**98.50**	**100**	**97.55**

methods require a proper selection of mother wavelets and several decomposition levels. The issues mentioned earlier will be overcome. By keeping aim to improve the classification accuracy, sensitivity, and specificity, a CNN-based model is proposed to achieve the highest ACCU, SENS, SPEC, and MACC values using testing data. In addition, the F1-score is also improved compared to state-of-the-art techniques that have utilized the AFAVA EEG dataset. Moreover, the comparison of the proposed method with the earlier existing methods using different EEG datasets is presented in Table 8. Alvi *et al.* [32] used spectral features from EEG signals and achieved classification accuracy of 96.91%. However, the hyperparameters of machine learning models were not optimized. The methods reported in [45–48] investigated the spectral and complexity features from the EEG signals and managed to obtain the 93.46 % accuracy. The proposed LCADNet model of AD detection improved the performance by 2% than existing methods.

4.2 Limitations and Future Directions

The proposed LCADNet outperformed the existing CNN models, but it still has some limitations. The proposed method has been employed on one publicly available AD EEG dataset. The population size of the datasets is relatively restricted. The LCADNet performance may further be improved by training with other AD EEG datasets. Several factors can affect a model's performance, such as age, gender, and use of medications. The EEG signals of AD patients

Table 8: Comparative analysis with earlier methods which have used ***different*** datasets.

Reference	Method	Ch	Subjects	Classifier	ACC (%)	SENS (%)	SPEC (%)
Geng *et al.* [46] (2022)	Spectral, complexity features	16	20 NC, 20 AD	GRU	93.46	93.33	93.60
Ding *et al.* [45] (2022)	Spectral, complexity, connectivity features	5	113 NC, 116 MCI, 72 AD	RUS boosting	72.43	65.28	76.99
Alvi *et al.* [32] (2022)	Spectrogram of EEG signals	19	11 NC, 16 AD	LSTM	96.91	97.95	96.16
Miltiadous *et al.* [29] (2023)	band power Spectral coherence connectivity	19	36 AD, 29 NC	Dual input CNN	83.28	78.81	87.94
Nour *et al.* [26] (2024)	Ensemble deep Learning model	19	24 AD, 24 NC	CNN	97.90	98.23	98.68
Siuly *et al.* [27] (2024)	PSD based biomarkers	20	31 AD1, 20 AD2, 35 NC	LSTM	97.00	97.48	96.48
This work (2024)	LCADNet model	16	11 NC, 12 AD	-	**98.50**	**100**	**97.55**

Ch-Number of EEG channels, LSTM -long short-term memory networks, GRU - Gated Recurrent Unit (GRU) is a type of RNN.

with lower age may perform well using the proposed model. However, medication and lower age group Alzheimer's disease patients can reduce the effect of Alzheimer's disease due to overlapping age-related issues in the EEG signals. The current study uses EEG recordings from both genders. No significant gender-specific performance variation was observed. In the future, the remaining concerns can be addressed per the availability of data. A CNN model is sensitive to variations in input data. While CNNs are highly effective in learning complex patterns from data, interpreting their internal representations and

understanding the decision-making process is challenging. Hence, the adoption of CNN models is formidable, where transparency and interpretability are crucial. Building on the foundations laid by this research, several directions for future work are:

- Expanding the dataset to include different demographics, ethnicities, and disease stages may enhance the generalizability of the proposed CNN model.
- Investigating the interpretation and visualization of CNN's decision-making process may make it more appealing for clinical adoption.
- A real-time implementation may enable continuous monitoring of disease and timely intervention, improving healthcare.
- Integrating EEG data with other medical data, such as neuroimaging or genetics, may enhance a comprehensive understanding of the disease.

Finally, extensive clinical validations need to assess the model's performance on a broader scale and ensure its practicality and safety for adoption in healthcare.

5 Conclusion

AD detection is a primary concern nowadays. To detect AD in its early stage is very urgent. Hence, this study proposed a novel and efficient AD detection model using a four-layer convolution network (LCADNet). LCADNet achieves the highest accuracy using two convolutional layers and two fully connected layers. LCADNet neural network is also compared to state-of-the-art DNN. The LCADNet outperforms the remaining respiratory sound type; it achieves 98.50% accuracy and 99.68% F1-score. The ability of the model can be generalized to effectively detect other neurological degenerative conditions. In conclusion, this research has made significant strides in the early detection of Alzheimer's Disease (AD) using EEG signals and CNNs. The study has highlighted the limitations of current clinical tests and hand-crafted feature-based methods for AD detection, emphasizing the need for more robust and objective approaches. The proposed configurable CNN architecture has demonstrated exceptional promise, achieving a maximum classification accuracy of 98.60%. Compared to other pre-trained models, its lower complexity makes it a strong candidate for practical applications in real-world healthcare settings. This work underscores the potential of machine learning and DL techniques to revolutionize the field of neurological disorder diagnosis, with implications extending beyond AD to conditions like epilepsy and sleep disorders.

In summary, this research paves the way for more accurate and objective methods for AD detection, with the potential to revolutionize the diagnosis and management of not only Alzheimer's Disease but also various other neurological conditions. Future work in this area holds promise for improving healthcare outcomes and advancing our understanding of neurological disorders.

Compliance with ethical standards

Conflict of Interest: The authors declare that there is no conflict of interest regarding this paper.
Ethical approval: This article contains no studies with human participants or animals performed by authors.
Informed consent: Informed consent was obtained from all individual participants included in the study.
Data availability statements: Data is available from the authors upon reasonable request.
Funding: Not Applicable

Authors Contribution

Pramod H. Kachare: Supervision, Methodology, Conceptualization, Writing - original draft. Digambar V. Puri: Software, Resources, Writing - original draft, Supervision, Methodology, Formal analysis, Review and editing. Sandeep B. Sangle: Software, Formal analysis, Writing - review and editing. Ibrahim Al-Shourbaji: Formal analysis, Writing - review and editing. Abdoh Jabbari: Formal analysis, Writing - review and editing. Raimund Kirner: Formal analysis, Writing - review and editing. Abdalla Alameen: Formal analysis, Writing - review and editing. Hazem Migdady: Formal analysis, Writing - review and editing. Laith Abualigah: Formal analysis, Writing - review and editing. All authors read and approved the final paper.

References

[1] Alzheimer's disease facts and figures. Alzheimer's and Dementia **16**(3), 391–460 (2020). https://doi.org/10.1002/alz.12068

[2] Jeong, J.: EEG dynamics in patients with Alzheimer's disease. Clinical Neurophysiology **115**(7), 1490–1505 (2004). https://doi.org/10.1016/j.clinph.2004.01.001

[3] Breijyeh, Z., Karaman, R.: Comprehensive review on Alzheimers Disease: Causes and Treatment. Molecules **25**(24) (2020). https://doi.org/10.3390/molecules25245789

[4] Puri, D.V., Nalbalwar, S.L., Nandgaonkar, A.B., Gawande, J.P., Wagh, A.: Automatic detection of Alzheimers disease from EEG signals using low-complexity orthogonal wavelet filter banks. Biomedical Signal Processing and Control **81**, 104439 (2023). https://doi.org/10.1016/j.bspc.2022.104439

[5] Modir, A., Shamekhi, S., Ghaderyan, P.: A systematic review and methodological analysis of EEG-based biomarkers of Alzheimer's disease. Measurement **220**, 113274 (2023). https://doi.org/10.1016/j.measurement.2023.113274

[6] Atri, A.: The Alzheimers Disease clinical spectrum: Diagnosis and management. Medical Clinics of North America **103**(2), 263–293 (2019). https://doi.org/10.1016/j.mcna.2018.10.009. Neurology for the Non-Neurologist

[7] Ghorbanian, P., Devilbiss, D., Hess, T., Bernstein, A., Simon, A., Ashrafiuon, H.: Exploration of EEG features of Alzheimers disease using continuous wavelet transform. Medical & Biological Engineering & Computing **53** (2015). https://doi.org/10.1007/s11517-015-1298-3

[8] Jiao, B., Li, R., Zhou, H., Qing, K., Liu, H., Pan, H., Lei, Y., Fu, W., Wang, X., Xiao, X., *et al.*: Neural biomarker diagnosis and prediction to mild cognitive impairment and Alzheimers disease using EEG technology. Alzheimer's research & therapy **15**(1), 1–14 (2023). https://doi.org/10.1186/s13195-023-01181-1

[9] Puri, D.V., Nalbalwar, S.L., Ingle, P.P.: EEG-Based Systematic Explainable Alzheimers Disease and Mild Cognitive Impairment Identification Using Novel Rational Dyadic Biorthogonal Wavelet Filter Banks. Circuits, Systems, and Signal Processing, 1–31 (2023)

[10] Lo Giudice, P., Mammone, N., Morabito, F., Pizzimenti, R., Ursino, D., Virgili, L.: Leveraging network analysis to support experts in their analyses of subjects with MCI and AD. Medical and Biological Engineering and Computing **57** (2019). https://doi.org/10.1007/s11517-019-02004-y

[11] Dauwels, J., Vialatte, F., Musha, T., Cichocki, A.: A comparative study of synchrony measures for the early diagnosis of Alzheimer's disease based on EEG. NeuroImage **49**(1), 668–693 (2010). https://doi.org/10.1016/j.neuroimage.2009.06.056

[12] Cassani, R., Falk, T.H., Fraga, F.J., Cecchi, M., Moore, D.K., Anghinah, R.: Towards automated electroencephalography-based Alzheimers disease diagnosis using portable low-density devices. Biomedical Signal Processing and Control **33**, 261–271 (2017). https://doi.org/10.1016/j.bspc.2016.12.009

[13] Al-nuaimi, A.H.H., Jammeh, E., Sun, L., Ifeachor, E.: Complexity Measures for Quantifying Changes in Electroencephalogram in Alzheimers Disease. Complexity **Vol. 2018 Article ID 8915079**, 1–12 (2018). https://doi.org/10.1155/2018/8915079

[14] Simons, S., Espino, P., Absolo, D.: Fuzzy Entropy Analysis of the Electroencephalogram in Patients with Alzheimers Disease: Is the Method Superior to Sample Entropy? Entropy **20**, 21 (2018). https://doi.org/10.3390/e20010021

[15] Puri, D., Nalbalwar, S., Nandgaonkar, A., Wagh, A.: EEG-Based Diagnosis of Alzheimer's Disease Using Kolmogorov Complexity. In: Applied Information Processing Systems, pp. 157–165. Springer, Singapore (2022)

[16] Ruiz-Gmez, S.J., Gmez, C., Poza, J., Gutirrez-Tobal, G.C., Tola-Arribas, M.A., Cano, M., Hornero, R.: Automated multiclass classification of spontaneous eeg activity in alzheimers disease and mild cognitive impairment. Entropy (2018) **20**(1) (2018). https://doi.org/10.3390/e20010035

[17] Abásolo, D., Hornero, R., Espino, P., Álvarez, D., Poza, J.: Entropy analysis of the EEG background activity in Alzheimer's disease patients. Physiological Measurement **27**(3), 241–253 (2006). https://doi.org/10.1088/0967-3334/27/3/003

[18] Fan, M., Yang, A., Fuh, J.-L., Chou, C.-A.: Topological Pattern Recognition of Severe Alzheimer's Disease via Regularized Supervised Learning of EEG Complexity. Frontiers in Neuroscience **12**, 685 (2018). https://doi.org/10.3389/fnins.2018.00685

[19] Azami, H., Absolo, D., Simons, S., Escudero, J.: Univariate and Multivariate Generalized Multiscale Entropy to Characterise EEG Signals in Alzheimers Disease. Entropy **19**(1), 1–17 (2017). https://doi.org/10.3390/e19010031

[20] Sharma, N., Kolekar, M.H., Jha, K., Kumar, Y.: EEG and Cognitive Biomarkers Based Mild Cognitive Impairment Diagnosis. IRBM **40**(2), 113–121 (2019). https://doi.org/10.1016/j.irbm.2018.11.007

[21] Durongbhan, P., Zhao, Y., Chen, L., Zis, P., De Marco, M., Unwin, Z.C., Venneri, A., He, X., Li, S., Zhao, Y., Blackburn, D.J., Sarrigiannis, P.G.: A Dementia Classification Framework using Frequency and Time-Frequency Features Based on EEG Signals. IEEE Transactions on Neural Systems and Rehabilitation Engineering **27**(5), 826–835 (2019). https://doi.org/10.1109/TNSRE.2019.2909100

[22] Farina, F.R., Emek-Sava, D.D., Rueda-Delgado, L., Boyle, R., Kiiski, H., Yener, G., Whelan, R.: A comparison of resting state EEG and structural MRI for classifying Alzheimers disease and mild cognitive impairment. NeuroImage **215**, 116795 (2020). https://doi.org/10.1016/j.neuroimage.2020.116795

[23] Oltu, B., Akahin, M.F., Kibarolu, S.: A novel electroencephalography

based approach for Alzheimers disease and mild cognitive impairment detection. Biomedical Signal Processing and Control **63**, 102223 (2021). https://doi.org/10.1016/j.bspc.2020.102223

[24] Pirrone, D., Weitschek, E., Di Paolo, P., De Salvo, S., De Cola, M.C.: EEG Signal Processing and Supervised Machine Learning to Early Diagnose Alzheimer's Disease. Applied Sciences **12**(11) (2022). https://doi.org/10.3390/app12115413

[25] Swarnalatha, R.: A Greedy Optimized Intelligent Framework for Early Detection of Alzheimers Disease Using EEG Signal. Computational Intelligence and Neuroscience **20**, 1–10 (2023). https://doi.org/10.1155/2023/4808841

[26] Nour, M., Senturk, U., Polat, K.: A novel hybrid model in the diagnosis and classification of Alzheimer's disease using EEG signals: Deep ensemble learning (DEL) approach. Biomedical Signal Processing and Control **89**, 105751 (2024). https://doi.org/10.1016/j.bspc.2023.105751

[27] Siuly, S., Alin, .F., Wang, H., Li, Y., Wen, P.: Exploring Rhythms and Channels-Based EEG Biomarkers for Early Detection of Alzheimer's Disease. IEEE Transactions on Emerging Topics in Computational Intelligence, 1–15 (2024). https://doi.org/10.1109/TETCI.2024.3353610

[28] Miltiadous, Andreas and Tzimourta, Katerina and Afrantou, Theodora and Ioannidis, Panagiotis and Grigoriadis, Nikolaos and Tsalikakis, Dimitrios and Angelidis, Pantelis and Tsipouras, Markos and Glavas, E. and Giannakeas, Nikolaos and Tzallas, Alexandros: A Dataset of Scalp EEG Recordings of Alzheimers Disease, Frontotemporal Dementia and Healthy Subjects from Routine EEG. Data **8**, 95 (2023). https://doi.org/10.3390/data8060095

[29] Calub, Gabriel Ivan A. and Elefante, Erickson N. and Galisanao, Jose Colin A. and Iguid, Sofia Lyn Beatrice G. and Salise, Jeremae C. and Prado, Seigfred V.: EEG-Based Classification of Stages of Alzheimers Disease (AD) and Mild Cognitive Impairment (MCI). In: 5th International Conference on Bio-engineering for Smart Technologies (BioSMART), pp. 1–6 (2023). https://doi.org/10.1109/BioSMART58455.2023.10162117

[30] Fouad, I.A., Labib, F.E.-Z.M.: Identification of Alzheimers disease from central lobe EEG signals utilizing machine learning and residual neural network. Biomedical Signal Processing and Control **86**, 105266 (2023). https://doi.org/10.1016/j.bspc.2023.105266

[31] Ho, T.K.K., Jeon, Y., Na, E., Ullah, Z., Kim, B.C., Lee, K.H., Song, J.-I., Gwak, J.: Deepadnet: A CNN-LSTM model for the multi-class classification of Alzheimers disease using multichannel EEG. Alzheimer's &

Dementia **17**, 057573 (2021)

[32] Alvi, A.M., Siuly, S., Wang, H.: A long short-term memory based framework for early detection of mild cognitive impairment from EEG signals. IEEE Transactions on Emerging Topics in Computational Intelligence, 1–14 (2022). https://doi.org/10.1109/TETCI.2022.3186180

[33] Toural, J.E., Maran Reyes, E.J.: Classification among healthy, mild cognitive impairment and Alzheimers disease subjects based on wavelet entropy and relative beta and theta power. Pattern Analysis and Applications **24** (2021). https://doi.org/10.1007/s10044-020-00910-8

[34] Simons, S., Absolo, D.: Distance-based LempelZiv complexity for the analysis of Electroencephalograms in patients with Alzheimers Disease. Entropy **19**, 129 (2017). https://doi.org/10.3390/e19030129

[35] Smith, K., Absolo, D., Escudero, J.: Accounting for the complex hierarchical topology of EEG phase-based functional connectivity in network binarisation. PloS one **12**(10), 0186164 (2017). https://doi.org/10.1371/journal.pone.0186164

[36] Al-Shourbaji, I., Kachare, P.H., Abualigah, L., Abdelhag, M.E., Elnaim, B., Anter, A.M., Gandomi, A.H.: A deep batch normalized convolution approach for improving covid-19 detection from chest x-ray images. Pathogens **12**(1) (2023). https://doi.org/10.3390/pathogens12010017

[37] Tharwat, A.: Classification assessment methods. Applied Computing and Informatics **17**, 168–192 (2021). https://doi.org/10.1016/j.aci.2018.08.003

[38] Puri, D.V., Gawande, J.P., Rajput, J.L., Nalbalwar, S.L.: A novel optimal wavelet filter banks for automated diagnosis of alzheimers disease and mild cognitive impairment using electroencephalogram signals. Decision Analytics Journal **9**, 100336 (2023). https://doi.org/10.1016/j.dajour.2023.100336

[39] Miltiadous, A., Gionanidis, E., Tzimourta, K.D., Giannakeas, N., Tzallas, A.T.: Dice-net: A novel convolution-transformer architecture for alzheimer detection in eeg signals. IEEE Access **11**, 71840–71858 (2023). https://doi.org/10.1109/ACCESS.2023.3294618

[40] Cejnek, M., Vyata, O., Valis, M., Bukovsky, I.: Novelty detection-based approach for Alzheimers disease and mild cognitive impairment diagnosis from EEG. Medical and Biological Engineering and Computing **59**, 1–10 (2021). https://doi.org/10.1007/s11517-021-02427-6

[41] Miltiadous, A., Tzimourta, K.D., Afrantou, T., Ioannidis, P., Grigoriadis,

N., Tsalikakis, D.G., Angelidis, P., Tsipouras, M.G., Glavas, E., Giannakeas, N., Tzallas, A.T.: A dataset of scalp eeg recordings of alzheimer disease, frontotemporal dementia and healthy subjects from routine eeg. Data **8**(6) (2023). https://doi.org/10.3390/data8060095

[42] Escudero, J., Abásolo, D., Hornero, R., Espino, P., López, M.: Analysis of electroencephalograms in Alzheimer's disease patients with multiscale entropy. Physiological Measurement **27**(11), 1091–1106 (2006). https://doi.org/10.1088/0967-3334/27/11/004

[43] Absolo, D., Hornero, R., Escudero, J., Espino, P.: A Study on the Possible Usefulness of Detrended Fluctuation Analysis of the Electroencephalogram Background Activity in Alzheimer's Disease. IEEE transactions on biomedical engineering **55**, 2171–9 (2008). https://doi.org/10.1109/TBME.2008.923145

[44] Simons, S., Abasolo, D., Escudero, J.: Classification of Alzheimer's disease from quadratic sample entropy of electroencephalogram. Healthcare Technology Letters **2**(3), 70–73 (2015). https://doi.org/10.1049/htl.2014.0106

[45] Ding, Y., Chu, Y., Liu, M., Ling, Z., Wang, S., Li, X., Li, Y.: Fully automated discrimination of Alzheimers disease using resting-state Electroencephalography signals. Quantitative Imaging in Medicine and Surgery **12**, 1063 (2022). https://doi.org/10.21037/qims-21-430

[46] Geng, D., Wang, C., Fu, Z., Zhang, Y., Yang, K., An, H.: Sleep EEG-Based Approach to Detect Mild Cognitive Impairment. Frontiers in Aging Neuroscience **14** (2022). https://doi.org/10.3389/fnagi.2022.865558

[47] Chedid, N., Tabbal, J., Kabbara, A., Allouch, S.: The development of an automated machine learning pipeline for the detection of Alzheimers Disease. Scientific Reports **12**, 18137 (2022). https://doi.org/10.1038/s41598-022-22979-3

[48] Puri, D., Nalbalwar, S., Nandgaonkar, A., Wagh, A.: Alzheimers disease detection with optimal EEG channel selection using wavelet transform. In: 2022 International Conference on Decision Aid Sciences and Applications (DASA), pp. 443–448 (2022). https://doi.org/10.1109/DASA54658.2022.9765166

[49] Absolo, D., Escudero, J., Hornero, R., Gmez, C., Espino, P.: Approximate entropy and auto mutual information analysis of the electroencephalogram in Alzheimer's disease patients. Medical and Biological Engineering and Computing **46**, 1019–28 (2008). https://doi.org/10.1007/s11517-008-0392-1

[50] Absolo, D., Hornero, R., Gmez, C., Escudero, J., Espino, P.: Electroencephalogram background activity characterization with Detrended Moving Average in Alzheimer's disease patients. 6^{th} IEEE International Symposium on Intelligent Signal Processing - Proceedings (2009) (2009). https://doi.org/10.1109/WISP.2009.5286531

[51] Puri, D., Nalbalwar, S., Nandgaonkar, A., Kachare, P., Rajput, J., Wagh, A.: Alzheimers Disease Detection using Empirical Mode Decomposition and Hjorth parameters of EEG signal. In: 2022 International Conference on Decision Aid Sciences and Applications (DASA), pp. 23–28 (2022). https://doi.org/10.1109/DASA54658.2022.9765111